

THE EFFECT OF COOLING RATE AND CERIUM MELT TREATMENT ON THERMAL ANALYSIS PARAMETERS AND MICROSTRUCTURE OF HYPOEUTECTIC Al-Si ALLOY

Vijeesh V and K Narayan Prabhu

Dept. of Metallurgical and Materials Engineering, National Institute of Technology Karnataka, Surathkal, Srinivasnagar, Mangalore 575025, India, e-mail: prabhukn_2002@yahoo.co.in

Keywords: Cerium, eutectic Si modification, chilling, thermal analysis

Abstract

In the present investigation, pure cerium ingots were added to Al-8% Si alloy melt to study its effect on the microstructure and cooling curve parameters. The melt treated alloy was solidified against sand base, stainless steel, brass, and copper chills to study the effect of chilling. Ce treated alloys solidified against sand base resulted in refinement of the eutectic silicon along with the formation of Al-Si-Ce ternary intermetallic compound. Addition of Ce to alloys solidified against chills resulted in the complete modification of eutectic silicon. Thermal analysis results revealed that the nucleation temperatures of eutectic silicon decreased on addition of cerium to the chilled alloys due to the synergistic effect of chilling and cerium addition. The degree of modification achieved was higher due to the decrease in the formation of Ce intermetallics at higher cooling rates.

List of symbols

1	$T_N(\alpha)$	α - Aluminum nucleation temperature
2	$T_{min}(\alpha)$	α - Aluminum minimum temperature
3	$T_G(\alpha)$	α - Aluminum growth temperature
4	$T_N(Eut)$	Eutectic silicon nucleation temperature
5	$T_{min}(Eut)$	Al-Si eutectic minimum temperature
6	$T_G(Eut)$	Al-Si eutectic growth temperature

1. Introduction

Aluminum-Silicon (Al-Si) alloys are most versatile materials, comprising 85% to 90% of the total aluminum cast parts produced for the automotive and aerospace industry. Depending on the Si concentration, the Al-Si alloy systems fall into three major categories: hypoeutectic (<12% Si), eutectic (12-13% Si) and hypereutectic (14-25% Si). The cast microstructure of hypoeutectic alloys consists of flake or needle like eutectic silicon in a eutectic matrix. The transformation of eutectic silicon into fine fibrous form enhances the mechanical properties of the alloy and the process is known as 'modification'. [1]. Generally, Group II elements are used to modify eutectic silicon in hypoeutectic Al-Si alloys. The modifying effect achieved by these elements faded in very short time and it had no effect on any other phase other than the eutectic Si in the alloy matrix. However, the strontium modification has longer fading time compared to sodium. In contrast, Sr in the melt increases the amount of hydrogen dissolved into the melt during holding time, which increases the number of pinholes in the castings [2]. Melt treatment of Al-Si alloys with rare-earth elements modified the eutectic Si with very less fading effect [3]. On the other hand, addition of rare-earth elements as misch-metal had a negative effect on hypoeutectic alloys, due to the grain coarsening effect. The mechanical properties were reduced although the eutectic silicon was completely modified [4].

The studies on the influence of elemental rare earth addition on silicon modification are limited. Since about 50-55 wt. % misch-

metal composition consist of cerium, it would be beneficial to study its effect on silicon modification. According to Lu and Hellawell [5] modification by chemical addition occurs by inducing twin in the silicon (Twin Plane Re-Edge (TPRE) mechanism). The modified silicon is heavily twinned compared to the unmodified silicon. The maximum twinning occurs when the ratio of atomic radius of the modifying agent and atomic radius of Si is closer to 1.65. The radii ratio (R_{Na}/R_{Si}) of sodium was 1.58, yet sodium produced fully modified structure at an addition of very low concentration of 0.01 Wt.%. Similar to sodium, the radii ratio (R_{Ce}/R_{Si}) for cerium against silicon is 1.56 and ideally cerium should modify eutectic silicon. The melt treatment of Al-Si alloys with cerium showed some effect on the eutectic silicon and α -aluminum. Nogita et al. [6] studied the effect of individual additions of rare earth metals on Al-10% Si alloy. The melt treated alloy with different rare earth elements at a temperature of 760°C (dissolution period of 40 min) was solidified in a tapered stainless tube at a cooling rate of 1 K/ min. The results showed that the rare earth elements such as cerium did not yield fully modified structure, however they resulted in refinement of the plate-like eutectic silicon. Voncina et al. [7] investigated the grain refining influence of Ce on A380 alloy. The alloy treated with pure cerium (99.9%) was cooled in a measuring cell with controlled cooling system. They studied the microstructures of the alloy with cerium addition solidified at varying cooling rates (10, 100, 300, 350 K/ min). It was reported that the addition of Ce at higher cooling rate resulted in the formation of smaller α -aluminum. Chen et al. [8] investigated the effect of Ce and Sr addition on the nucleation kinetics of α -aluminum. They reported decrease in the activation energy of α -aluminum on addition of Ce. Asmael et al. [9] studied the effect of Ce addition on near eutectic Al-11.7% Si alloy. The melt at 750 °C was treated with elemental pure cerium and solidified in a preheated ceramic mould. The results showed a decrease in the nucleation and growth temperatures, along with the refinement in silicon particle with the addition of Ce.

There is no significant research work on cerium modification of and the assessment of the combined effect of cerium addition and chilling on morphology of eutectic silicon has yet been studied. The present study aims to investigate the effect of cerium addition and different chilling conditions on cooling curve parameters and microstructure of Al-8% Si.

2. Experimental Details

Al-8%Si-2%Cu-0.5%Mg-0.25%Fe alloy was used in the present study. About 350±50g of the alloy sample was melted in a clay-graphite crucible using an electrical resistance furnace. The alloy was treated with Cerium (Alfa Aesar, Cerium ingot, 99% pure (REO)) and strontium (Al-10Sr master alloy) in varying quantities at 750°C. The holding time was 30 minutes at 750°C. The melt was then poured to a stainless tube with/without chill at the bottom. Figure 1 shows the experiment set-up used for the study. A stainless steel tube of 50 mm outer diameter and 1 mm wall thickness instrumented with a chill at the bottom was selected for

pouring of the liquid metal. Stainless steel tube was selected as it has low thermal conductivity (16 W/mK). Copper, brass and stainless steel chills having varying thermal conductivities were selected to obtain different cooling rates. The surface roughness of all the chills was maintained at $0.5 \pm 0.05 \mu\text{m}$. To maintain constant cooling conditions, the stainless steel tube was covered with a ceramic insulation blanket. The temperature data from the casting was recorded during solidification using a K-type thermocouple connected to a high-speed data acquisition system (NI USB 9162) interfaced with a PC.

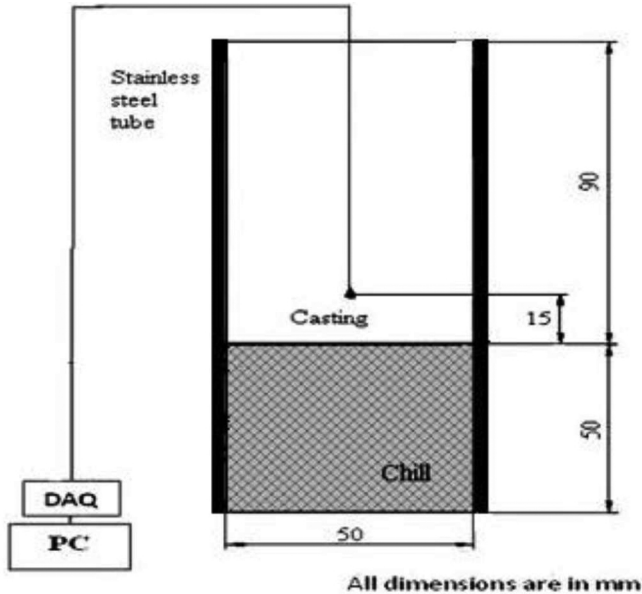


Figure 1 Schematic sketch of solidification setup

For microstructure studies, samples of 15 mm in diameter, and 15 mm in height were cut from the central portion of castings and samples were polished using silicon carbide papers of varying grit sizes of 180, 220, 400, 800, and 1000- μm . The final polishing was done using a rotating disc polisher with $0.3 \mu\text{m}$ levigated alumina. Microstructures of specimens were examined under JEOL JSM-6380LA scanning electron microscope. The silicon particle size was measured using Axio Vision image analysis software. The eutectic Si characteristics like area, length, perimeter, aspect ratio (length/width) and roundness factor ($P^2/4\pi A$, where, P is perimeter and A is the area of silicon particle) were measured at different locations of samples.

3. Results and Discussion

3.1 Microstructure analysis

Figure 2(a) shows the micrograph of an unchilled Al-8% Si alloy cast sample. The microstructure consists of long needle-like eutectic silicon in a matrix of pro-eutectic α -aluminum. Figure 2 (b) shows the presence of α -AlFeSi intermetallic with a Chinese script morphology in the alloy. Figure 3 shows the microstructure of the alloy after the addition of cerium. The addition of Ce had transformed the eutectic Si into short rod-like particles. The microstructures also shows the presence of a Ce based intermetallic compound formed due to the addition of Ce. With increase in Ce content, the morphology of the intermetallic formed transformed from needle-like particles into block-like particles.

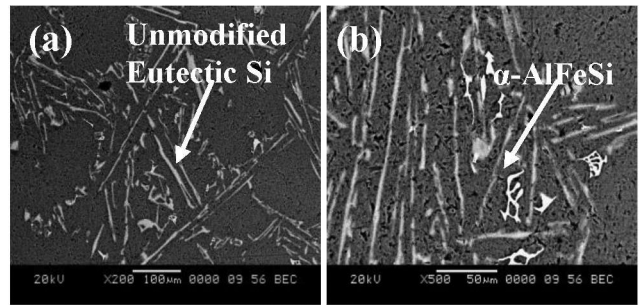


Figure 2 Microstructure of unchilled Al-8%Si alloy

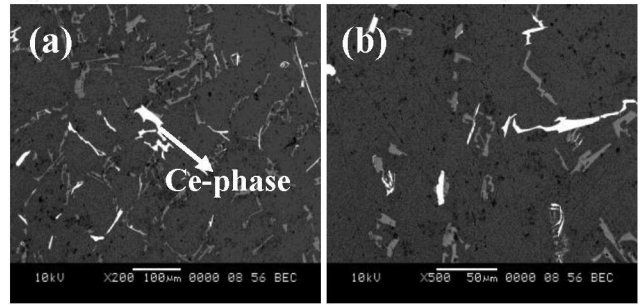


Figure 3 Microstructure of unchilled alloys with 1.5wt%-Ce addition

The particle characteristics such as length, width, area and perimeter of the Si particles were measured using Axio-vision software. The results of the particle characteristics of unchilled alloys with and without Ce additions are given in Table 1. The spherical nature of the eutectic Si particle was assessed by the roundness factor and the aspect ratio (Table 1). A roundness factor and aspect ratio of 1 indicates that the particle is a perfect sphere. According to the results, the untreated alloy showed higher values of Si particle characteristics (length, area, and perimeter) and a roundness value. The Si particle characteristics decreased with the addition of cerium. For example, the characteristic length ($4A/P$) of the untreated silicon was $65 \pm 30 \mu\text{m}$ and with the addition of 2 %, Ce, the length decreased to $28 \pm 15 \mu\text{m}$, showing a 56% reduction in the size.

Table 1 Eutectic silicon particle characteristics of unchilled alloy

Ce/wt-%	Length (μm)	Aspect ratio	Area (μm^2)	Perimeter (μm)	Roundness factor
0.0	65.0 ± 30	12.5	225.0 ± 150	138.0 ± 92	6.7
0.5	50.0 ± 15	9.4	206.0 ± 98	130.0 ± 33	6.5
1.0	47.5 ± 20	9.0	241.0 ± 120	121.0 ± 38	4.8
1.5	29.5 ± 18	6.6	112.0 ± 65	76.0 ± 30	4.1
2.0	28.0 ± 18	6.4	92.0 ± 50	70.0 ± 25	4.2

Similarly, the aspect ratio of the particle also decreased with the addition of Ce. This indicates that the Si particles are refined with the addition of Ce. The spherical nature of the particle was assessed by the roundness factor. The roundness factor approaches unity as the particle becomes spherical. The untreated alloy solidified against sand base showed a roundness factor above 6, indicating the acicular nature of the Si particles formed. The addition of Ce decreased the roundness factor. For example, with addition of 2% Ce, the roundness factor decreased to 4.2.

Figure 4 shows the effect of chilling on the microstructure of untreated alloy. Figure 5 shows the silicon particle characteristics of the alloys solidified on various chills. The results indicate that the untreated alloys solidified against chills showed a significant decrease in the particle characteristics compared to the slowly cooled alloys. Chilling marginally affected the acicular nature of the eutectic Si. The silicon particle size decreased with the increase in the thermal conductivity of the chill. The characteristic length of eutectic Si in copper, brass, and stainless steel chilled alloys were 16.6, 20.5, and 26.5 μm respectively. The roundness factors of untreated chilled alloys were around 5.5. This was marginally lower than that obtained with unchilled alloy. This indicates that the acicular nature of the Si particles were least affected by chilling although the eutectic Si was refined.

Figure 6 shows the effect of cerium addition on microstructure of alloys solidified against different chills. The silicon particle characteristics at different solidifying conditions for varying Ce content are shown in Figure 5 (a and b). According to the results, the addition of Ce had a significant affect on the Si particle characteristics of chilled alloys. The decrease in particle characteristics was mainly due to the combined effect of chilling and Ce modification. The Si particle size decreased significantly by about 87% compared to the untreated unchilled alloy. The silicon characteristic lengths were lowest at 2 % Ce addition and were 8.4, 7.9, and 8.5 μm respectively for copper, brass and stainless steel chills. Most importantly, the roundness factor also decreased significantly, to a low value of 1.7 due to the synergistic effect of chilling and cerium addition. Due to the addition of Ce to chilled alloys, the acicular Si particles had transformed into nearly spherical particles resulting in modified fine fibrous structure. The result also indicates that the extent of modification increases with the cooling rate. For example, the roundness factor of 2% cerium added alloy solidified on copper chill was less than the roundness factor of the alloy solidified on stainless steel.

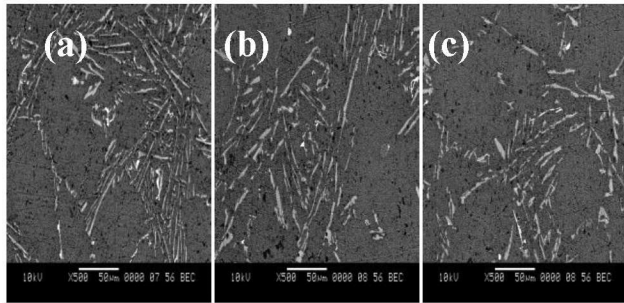


Figure 4 Microstructures of Al-8% Si alloy solidified against different chills (a) copper (b) brass (c) stainless steel

3.2 Thermal analysis

Figure 7 shows the cooling and first derivative curves of unchilled Al-8 % Si alloy. In order to illustrate the various arrest points, the temperature characteristics of different phases are shown in the figure. The pro-eutectic aluminum and eutectic silicon nucleation temperatures of untreated alloy are 602°C and 564°C respectively. Figure 8 shows the effect of cerium addition on cooling curve of the alloy for various solidifying conditions. The effects of addition of Ce on cooling curve parameters were assessed using the temperature characteristics such as T_{min} and T_G .

Table 2 shows the thermal analysis parameters of the alloy for

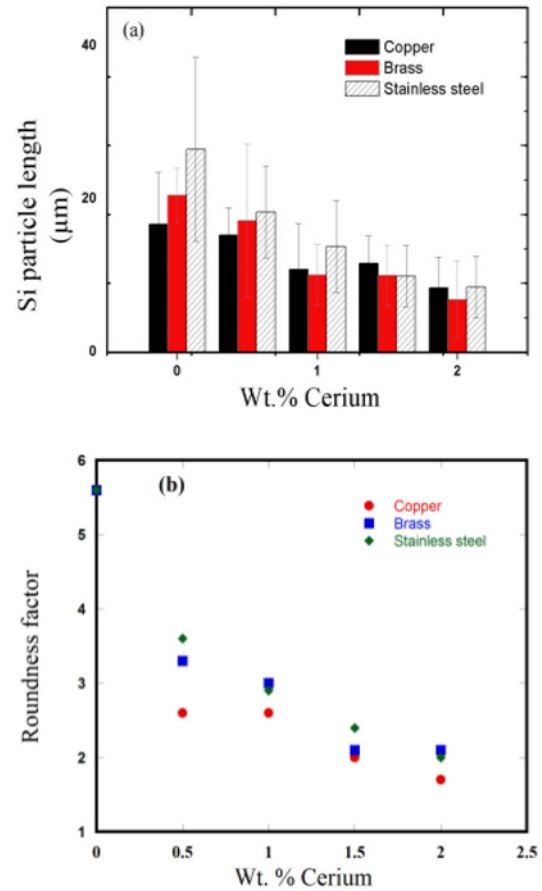


Figure 5 Variation of silicon particle characteristic with addition of Ce and cooling rate (a) silicon characteristic length (b) roundness factor

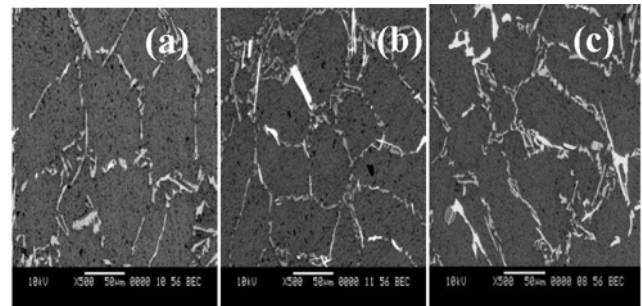


Figure 6 Microstructures of Ce modified Al-8%Si alloy solidified against different chills (a) copper (b) brass (c) stainless steel

different solidifying conditions. Nucleation temperature of the alloy decreased with the increase in Ce content for all conditions except for unchilled alloys. The results indicate that for unchilled alloys and low concentration (0.5%) of Ce, α -aluminum nucleation temperature increased by about 8°C and then decreased with further addition. Similarly, the eutectic nucleation temperature also increased with cerium addition. According to Grobner et al [10] in an Al-Ce-Si system for low concentration of Ce only two phases r_1 [$\text{Ce}(\text{Si}_{1-x}\text{Al}_x)_2$] and r_2 [AlCeSi_2] are thermodynamically stable. Hence, in the present study either of these two phases might have formed during solidification and would have acted as nucleant for α -aluminum phase leading to an

increase in nucleation temperatures. Figure 3(b) shows the presence of Al-Si-Ce phase in the alloy formed due to the addition of Ce. Previous studies by authors [11] show that the morphology and composition of the Al-Si-Ce formed varies with the cerium content and cooling rate. The variation in the morphology and composition of Al-Ce-Si intermetallic formed is the prime reason for the decrease in α - nucleation temperature with increase in Ce content.

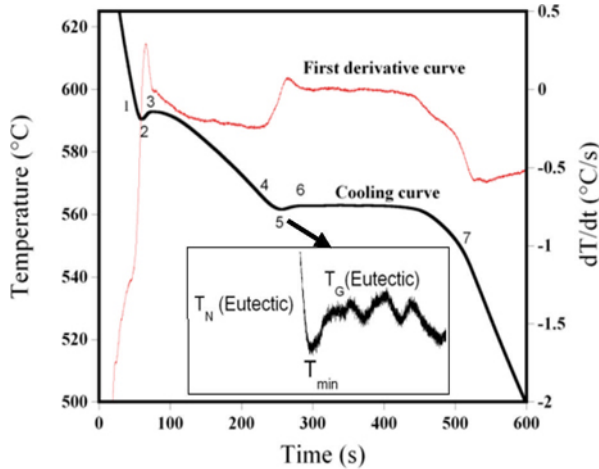


Figure 7 Cooling and first derivative curve for Al-8 % Si alloy

In the case of chilled alloys, the nucleation temperatures decreased with increase in thermal conductivity of the chill and cerium content. The eutectic minimum temperature T_{min} (Eut) of untreated alloys solidified on copper, brass, and stainless steel were 559.7, 561.0, and 561.5 °C respectively. With 2% Ce addition, the T_{min} (Eut) of the alloy decreased to 554, 558.2, and 557.3 °C for copper, brass, and stainless steel respectively. The eutectic growth temperature difference (ΔT_G) parameter was used to quantify the effect of Ce addition on thermal parameters for varying solidifying conditions.

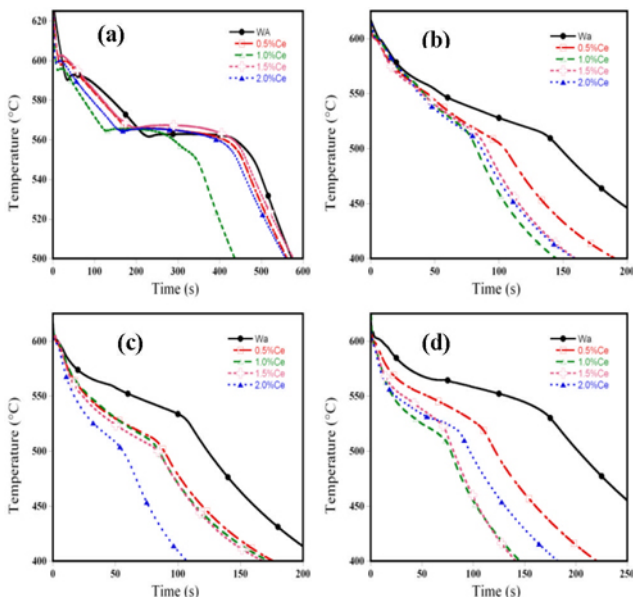


Figure 8 Cooling curves of the alloys with varying Ce content solidified on (a) unchilled (b) copper (c) brass and (d) stainless steel chills

Table 2 Effect of Ce addition on cooling curve parameters of Al-8% Si alloy at different solidifying conditions

	Ce wt-%	T_N (α) (°C)	T_{min} (α) (°C)	T_G (α) (°C)	T_N (Eut) (°C)	T_{min} (Eut) (°C)	T_G (Eut) (°C)
Unchilled	0.0	602.9	590.2	592.4	564	562	563.2
	0.5	610.9	592.5	594	566.4	564.2	565.2
	1.0	607.7	595.6	596.2	566.1	564.4	565.4
	1.5	603.2	601.9	602.6	568.2	566.4	567.4
	2.0	602.6	598.4	600	566.3	564.5	565.6
Copper	0.0	599.3	598.7	599.1	561	559.7	559.2
	0.5	602.8	601.4	600.1	562	559.6	556.2
	1.0	602.4	602	602.8	561.8	559	556
	1.5	601.3	600.1	600.5	561.2	558.2	555.2
	2.0	601.2	600.1	599.7	556.8	554	554.2
Brass	0.0	599.4	599.2	599.5	562.7	561.0	561.2
	0.5	600.5	598.6	597.4	561.8	560.2	557.7
	1.0	601.7	601.2	600.3	561.4	560.2	556.8
	1.5	603.6	603	602.5	560.2	559.2	556.5
	2.0	599.8	599.2	598.5	559.5	558.2	556.2
S. steel	0.0	596.1	594.5	592.1	562.1	561.5	561.9
	0.5	600.9	596.8	595.8	562.5	560.9	560.1
	1.0	601.7	600.4	599.7	562.2	559.1	557.2
	1.5	601.2	599.4	598.4	559.5	556.2	555.1
	2.0	601.7	598	597.7	558.1	557.3	555.3

Figure 9 shows the variation of ΔT_G with Ce addition. The ΔT_G values increased with the addition of Ce to the chilled alloys. Compared to unchilled alloys, the chilled alloys showed a significant decrease in growth temperatures. The growth temperature increased with the addition of Ce in the case of unchilled alloys and ΔT_G values increased marginally. The decrease in growth temperature was correlated with the degree of eutectic Si modification. Higher the ΔT_G value, higher is the Si modification. In the present study, the ΔT_G increased with the thermal conductivity of the chill and with cerium content. The copper chilled alloy showed a maximum ΔT_G of 9 at 2% Ce, corresponding to complete modification of eutectic Si.

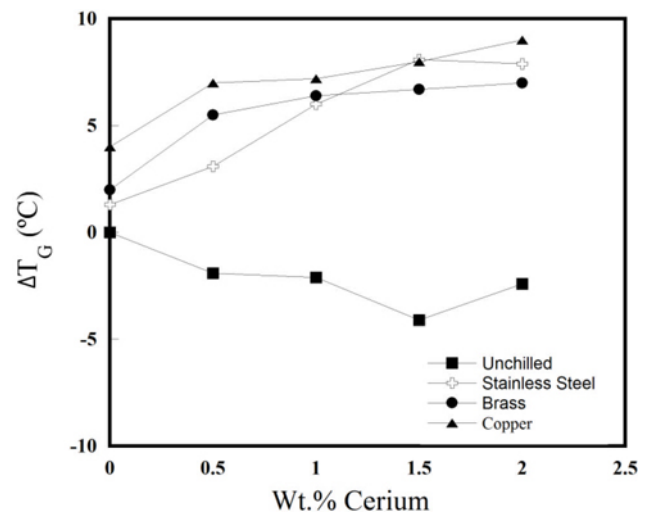


Figure 9 Variation of growth temperature difference with the addition of cerium for different solidifying conditions additions. The higher degree of silicon modification achieved by Ce melt treatment was due to the ability of Ce atom in adsorbing into Si

twin re-entrant groove and in preventing the growth of the silicon. As a result, the decrease in growth temperature led to the modification of the eutectic Si. At slow cooling conditions, the Ce atoms combine with Al and Si to form Al-Si-Ce ternary compound and which prevents complete modification of eutectic Si. At high cooling rates, the fast moving solidification front hinders the movement of Ce atoms. As a result, less number of Ce-intermetallics are formed and the presence of the Ce atoms in the eutectic matrix would lead to the modification of eutectic Si.

4. Conclusion

The effect of cooling rate and Ce melt treatment on microstructure and thermal analysis parameters were studied during solidification of Al-8% Si alloy. Based on the results, the following conclusions were drawn.

- Addition of elemental cerium to unchilled alloys did not modify the eutectic silicon. The eutectic silicon was modified partially. In the case of chilled alloys, due to the synergistic effect of chilling and Ce addition, the eutectic Si was completely modified.
- The microstructure of Ce modified alloys showed the presence of blocky shaped Al-Si-Ce ternary intermetallic formed due to the addition of Ce. The concentration of the Ce phase decreased with increase in cooling rate.
- Thermal analysis results showed that the addition of Ce had significant effect on the nucleation temperatures of α -aluminum and eutectic silicon phases. The nucleation temperatures of α -aluminum and eutectic Si increased on addition of Ce to unchilled alloys, whereas, the nucleation temperatures decreased with Ce addition to chilled alloys. The eutectic growth temperature difference (ΔT_G) decreased significantly due to the combined effect of chilling and addition of Ce.

Acknowledgements

V Vijeesh thanks National Institute of Technology Karnataka (NITK) Surathkal, Mangalore, India for the Research Scholarship. The authors acknowledge the help received during casting process from Mr Sathish and Mr Dinesha, Technicians at the Department of Metallurgical and Materials Engineering, National Institute of Technology Karnataka, Surathkal, India. The authors also thank Ms Rashmi Banjan, SEM operator, National Institute of Technology Karnataka (NITK), Surathkal, India, for her assistance during scanning electron microscopy.

5. References

1. S. Hegde, and K. N. Prabhu, "Modification of eutectic silicon in Al-Si alloys," *J. Mater. Sci.*, 43(2008), 3009-3027.
2. John E. Gruzleski, and Bernard M. Closset, *The treatment of liquid aluminum-silicon Alloys* (Des Plaines, Illinois: American Foundrymen's Society, Inc.,1990) 1-20.
3. T. Duo-guang, and M. Xie-min, "A new approach to refining and modifying cast aluminum alloys with rare earth alloys," *Journal of Shanghai University (English Edition)* 4(2) (2000), 167-170.
4. M. Zhu, Z. Jian, L. Yao, C. Liu, G. Yang, and Y. Zhou, "Effect of mischmetal modification treatment on the microstructure, tensile properties, and fracture behavior of Al-7.0%Si-0.3%Mg foundry aluminum alloys," *J. Mater. Sci.* 46(2011), 2685-2694.

5. S. Lu, and A. Hellawell, "Growth mechanisms of silicon in Al-Si alloys," *J. Cryst. Growth*, 73(1985), 316-328.
6. K. Nogita, S.D. McDonald, and A. K. Dahle, "Eutectic modification of Al-Si alloys with rare earth metals," *Materials Transactions*, 45(2)(2004), 323-326.
7. M. Voncina, P. Mrvar, M. Petric, and J. Medved, "Microstructure and grain refining performance of Ce on A380 alloy," *J. Min. Metall. Sect. B-Metall.* 48 (2) (2012) 264 - 272
8. Chen, X. Hao, J. Zhao, and C. Ma, "Kinetic nucleation of primary α -Al dendrites in Al-7% Si Mg cast alloys with Ce and Sr additions," *Trans. Nonferrous Met. Soc. China* 23(2013), 3561-3567
9. M. B. A. Asmael, R. Ahmad, A. Ourdjini, and S. Farahany, "Effect of elements cerium and lanthanum on eutectic solidification of Al-Si-Cu near eutectic cast alloy," *Advanced Materials Research*, 845 (2014), 118-122.
10. Grobner, J., Mirkovic, D. and Schmid-Fetzer, R., (2004) "Thermodynamic aspects of the constitution, grain refining and solidification enthalpies of Al-Ce-Si alloys," *Metall. Mater. Trans. A*, Vol. 35A, pp.3349-3362.
11. V. Vijayan and K N. Prabhu *Canadian Metallurgical Quarterly* 2014 Doi:10.1179/1879139514Y.0000000151